MAPPING AND PREDICTING THE IONOSPHERE

Stefan Schaer, Gerhard Beutler, Markus Rothacher
Astronomical Institute, University of Berne
CH-3012 Berne, Switzerland

ABSTRACT

The Center for Orbit Determination in Europe (CODE) produces daily maps of the Earth's ionosphere on a regular basis since January 1, 1996. These global ionosphere maps (GIMs) are derived from exactly the same GPS tracking data — doubly differenced carrier phase measurements — as those used for the determination of CODE core products delivered to the IGS like precise GPS orbits, earth orientation parameters (EOPs), station coordinates and velocities. For the ionospheric product we have to analyze the so-called *geometry*-free linear combination (LC), which primarily contains ionospheric information, as opposed to the *ionosphere*-free LC, which contains the "geometrical" information and completely eliminates the influence of the ionospheric refraction (ignoring higher-order terms). At present (March 1998), the GPS tracking network processed at CODE consists of more than 110 globally distributed stations of the International GPS Service for Geodynamics (IGS).

After reprocessing all 1995 IGS data using the "Bernese Processing Engine" [Rothacher et al., 1996a], a long-time series of daily GIM parameters covering a time span of about 3.2 years is at our disposal. On the one hand this ionosphere time series reveals the evolution of the total electron content (TEC) on a global scale, on the other hand it indicates that *short*-term as well as *long*-term predictions for CODE GIM parameters are possible. We discuss the time series for a few selected TEC parameters and develop a method to predict the TEC parameters. Futhermore, we describe how the temporal resolution can be increased when using spherical harmonic (SH) expansions to model the global TEC. First attempts estimating 2-hour maps are encouraging.

CODE'S IONOSPHERE PRODUCTS — AN OVERVIEW

The principles of the TEC mapping technique used at CODE were described in [Schaer et at., 1995] and [Schaer et al., 1996a].

At present the following ionosphere products are generated on a routine basis:

- 24-hour global ionosphere maps (GIMs) are produced using double-difference phase *or* phase-smoothed code observations. The *phase*-derived TEC maps proved their usefulness for ambiguity resolution (AR) on long baselines [Rothacher et al., 1996b].
- *Rapid* global maps are available with a delay of about 12 hours, the *final* ones after 3 days (in the IONEX format [Schaer et al., 1998]).
- Regional (European) maps are produced as well and are also used to support AR. On the average 90% of the initial carrier phase ambiguities can be resolved reliably — without making use of code measurements. Daily IONEX files containing hourly snapshots of the ionosphere are made available via anonymous ftp.
- Daily sets of differential code biases (DCBs) for all GPS satellites (and the contributing receivers) are estimated at CODE since October 1997.

Figure 1 shows the daily DCB estimates (dots) for 27 GPS satellites from day 022, 1998, to day 071, 1998, and the combined DCBs (circles) aligning all satellite-specific DCBs in the sense that the overall mean becomes *zero* (to obtain a virtual, but very stable reference). However, there are a couple of PRNs with *drifting* DCBs with respect to the remaining PRNs. PRN 08, which was launched few months ago, shows a significant drift of almost -0.5 ns over 50 days. We observe an increased root-mean-square error (RMS) for this satellite when assuming and modeling the DCBs as constant quantities (see Figure 1 and Table 1).

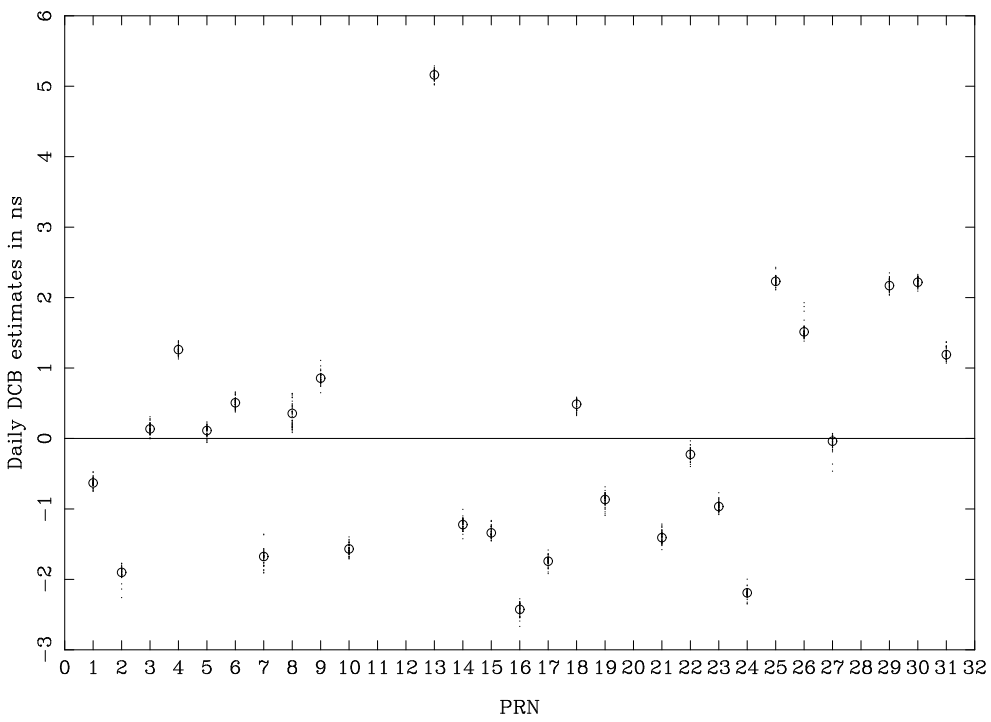

Figure 1. Daily PRN-specific DCB estimates (dots) for 27 GPS satellites from day 022, 1998, to day 071, 1998, and combined DCBs (circles)

The *combined* values of the satellite-specific DCBs taking into account the variance information of the individual solutions are listed in Table 1. In addition, the weighted RMS (WRMS) of the daily estimation is given for each PRN. The total WRMS of the 50-day DCB combination amounts to 0.08 ns. Let us mention that the estimated *receiver-specific* DCBs are of the order of ±15 ns and show a day-to-day scattering highly depending on the station considered. Note that the DCB results presented here originate from a special solution where we simultaneously estimate n station-specific TEC models leading to $16\,n$ TEC plus $n + 27$ DCB parameters per day in total, where n is the number of stations processed.

Table 1. Combined DCBs and weighted RMS errors of daily estimation

PRN	DCB (ns)	WRMS (ns)	PRN	DCB (ns)	WRMS (ns)
01	−0.63	0.06	17	−1.74	0.06
02	−1.90	0.07	18	+0.49	0.07
03	+0.14	0.06	19	−0.87	0.08
04	+1.26	0.06	21	−1.41	0.08
05	+0.11	0.07	22	−0.23	0.06
06	+0.51	0.07	23	−0.97	0.06
07	−1.68	0.11	24	−2.19	0.06
08	+0.35	0.16	25	+2.23	0.05
09	+0.86	0.07	26	+1.51	0.09
10	−1.57	0.07	27	−0.04	0.08
13	+5.16	0.06	29	+2.17	0.07
14	−1.22	0.07	30	+2.22	0.06
15	−1.34	0.07	31	+1.19	0.07
16	−2.43	0.08			

Figure 2 shows snapshots of (a) a *phase*-derived and (b) a *code*-derived 24-hour TEC map for day 017, 1998 (taken at 12:00 UT). The number of contributing stations was 79 on that particular day. Light fields indicate small TEC, dark ones large TEC (up to 37.6 and 39.0 TECU here). The level lines are drawn at intervals of 2.5 TECU. There is no significant difference between the two maps.

LONG-TIME SERIES OF GLOBAL TEC PARAMETERS

The long-time series of global TEC parameters available at CODE covers over 1168 days and includes $(8 + 1)^2 = 81$ SH coefficients (the SH expansion was truncated at degree and order 8). The zero-degree SH coefficient representing the mean TEC on a global scale characterizes the ionospheric activity pretty well. The evolution of this particular TEC parameter during a period of low solar activity is shown in Figure 3. The daily estimates (dots) and a smoothed curve to better visualize the behavior are given. One recognizes a long-term trend caused by the 11-year solar cycle, annual and semi-annual variations, and relatively strong short-term fluctuations with periods of the order of 27 days due to the Sun's rotation. We clearly see maxima at equinox and minima at solstice, however, the minima in summer are more pronounced than those in winter. The recent ionospheric minimum was observed in summer 1996.

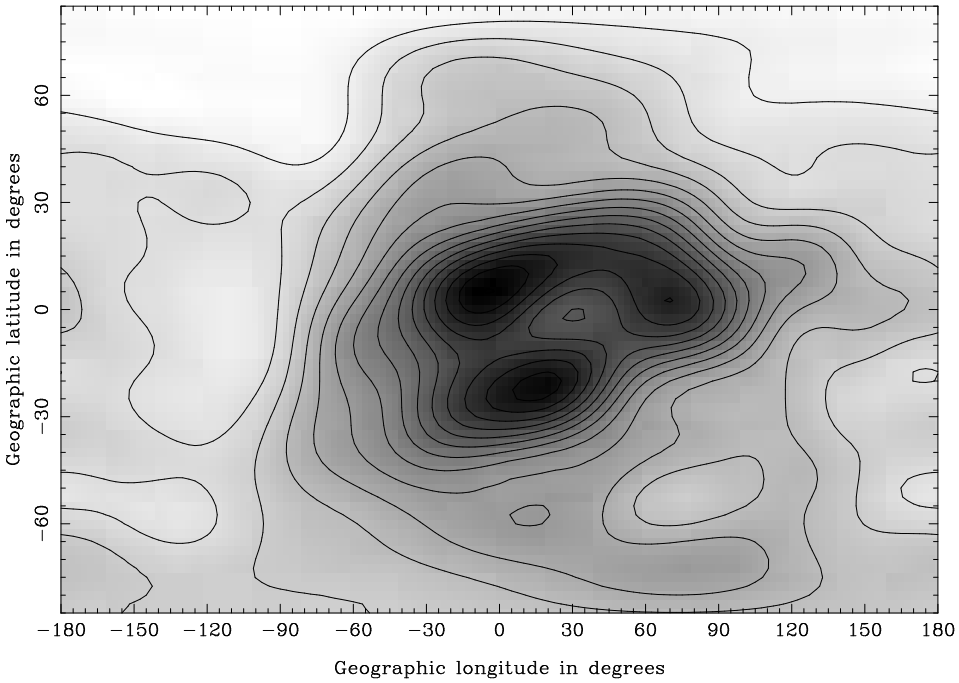

(a) *Phase*-derived TEC map

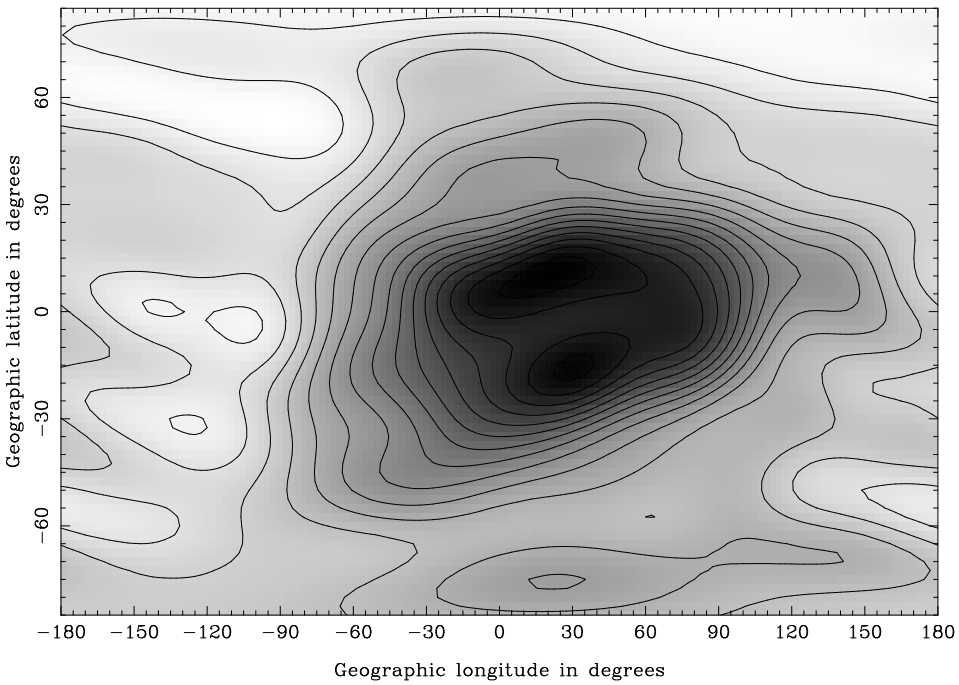

(b) *Code*-derived TEC map

Figure 2. 24-hour TEC maps for day 017, 1998

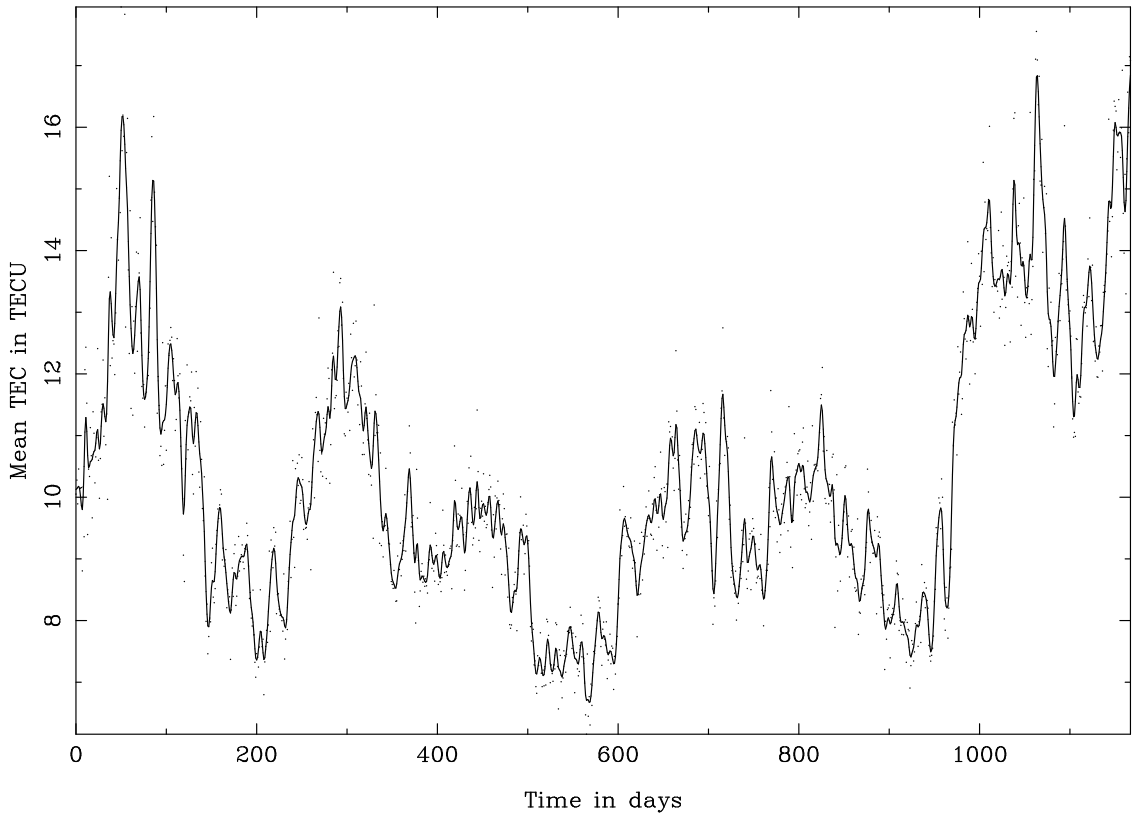

Figure 3. Zero-degree coefficient (mean TEC) from day 001, 1995 to day 072, 1998

Figures 4 and 5 illustrate a few other SH coefficients showing similar periodicities and features as mentioned above.

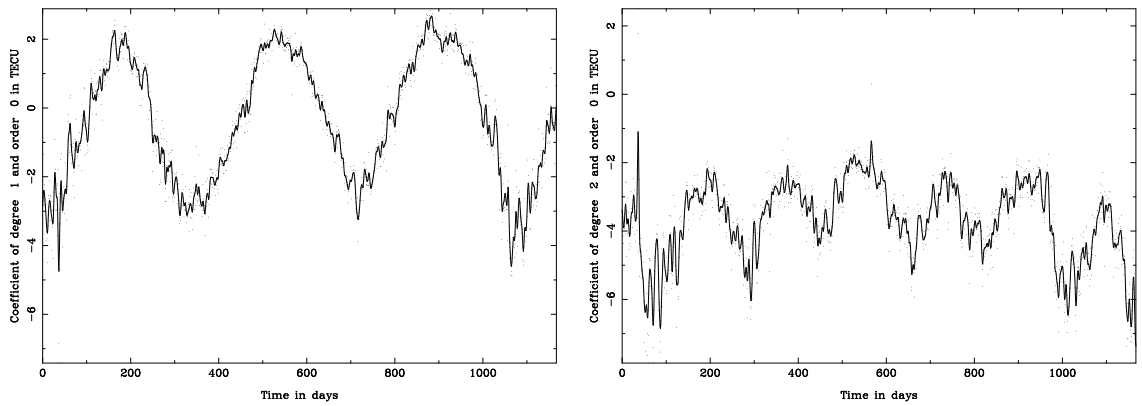

(a) Term of degree 1 (and order 0)

(b) Term of degree 2 (and order 0)

Figure 4. Zonal SH terms

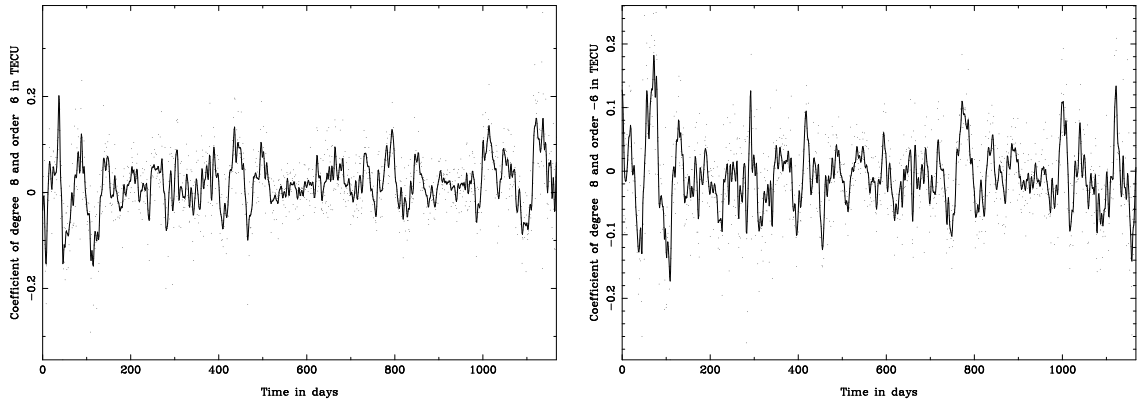

(a) Cosine term of degree 8 and order 6

(b) Sine term of degree 8 and order 6

Figure 5. Tesseral SH terms

When correlating the mean TEC values and the 10.7-cm solar flux, the correlation factor is almost 0.8, reaching its maximum at a lag of 1 day.

PREDICTING THE IONOSPHERE

Let us split up the "ionospheric signal" $\boldsymbol{l}$ — a time series of SH TEC parameters $e_{ij}(t_k)$ — into a *deterministic* component $\boldsymbol{d}$, which can be represented by a so-called trend function $\Phi(t)$, a *stochastic* component $\boldsymbol{s}$, and a noise component $\boldsymbol{n}$:

$$\boldsymbol{l} = \boldsymbol{d} + \boldsymbol{s} + \boldsymbol{n} \quad \text{or} \quad \boldsymbol{l} - \boldsymbol{\Phi}(\boldsymbol{x}_0) = \boldsymbol{A}\,\boldsymbol{x} + \boldsymbol{s} + \boldsymbol{n}. \tag{1}$$

As our trend function we use a harmonic expansion with a few prominent periods (11, 1, and 1/2 years)

$$\Phi(t) = a_0 + \sum_{i=1}^{m} \left(a_i\, \cos(\omega_i\, t) + b_i\, \sin(\omega_i\, t)\right) \quad \text{with} \quad \omega_i = \frac{2\,\pi}{\tau_i}. \tag{2}$$

The unknown parameters $\boldsymbol{x}$ of the trend function are estimated in a least-squares adjustment

$$\boldsymbol{x} = \left(\boldsymbol{A}^T\, \boldsymbol{C}_{zz}^{-1}\, \boldsymbol{A}\right)^{-1}\, \boldsymbol{A}^T\, \boldsymbol{C}_{zz}^{-1}\, \left(\boldsymbol{l} - \boldsymbol{\Phi}(\boldsymbol{x}_0)\right), \tag{3}$$

where

$$\boldsymbol{x}^T = [a_0, a_1, b_1, \ldots, a_n, b_n] \quad \text{and} \quad \boldsymbol{C}_{zz} = \boldsymbol{C}_{ss} + \boldsymbol{C}_{nn}. \tag{4}$$

$\boldsymbol{C}_{ss}$ and $\boldsymbol{C}_{nn}$ are the covariance matrices for the actual "signal" and the pure "noise", respectively. Finally, if we perform short-term predictions (or interpolations), the *stochastic* component $\boldsymbol{s}$ is of interest, too:

$$\begin{bmatrix} \boldsymbol{s} \\ \boldsymbol{n} \end{bmatrix} = \begin{bmatrix} \boldsymbol{C}_{ss} \\ \boldsymbol{C}_{nn} \end{bmatrix} \boldsymbol{C}_{zz}^{-1} \, (\boldsymbol{l} - \boldsymbol{\Phi}(\boldsymbol{x})) \,. \tag{5}$$

The autocovariance function γ, which is used to set up the covariance matrices $\boldsymbol{C}_{ss}$ and $\boldsymbol{C}_{zz}$, may be evaluated as

$$\gamma(h\,\Delta t) = \frac{1}{n} \sum_{k=1}^{n-|h|} (e_{ij}(t_k) - \Phi(t_k)) \, (e_{ij}(t_{k+|h|}) - \Phi(t_{k+|h|})). \tag{6}$$

$h\,\Delta t$ denotes the lag; $\gamma(0)$ is the variance of the stochastic component.

The autocovariance function (ACF) of the mean TEC, i. e., the SH coefficient e_{00}, is given in Figure 6. We notice that the ACF mainly reflects the Sun's rotation period of approximately 27 days.

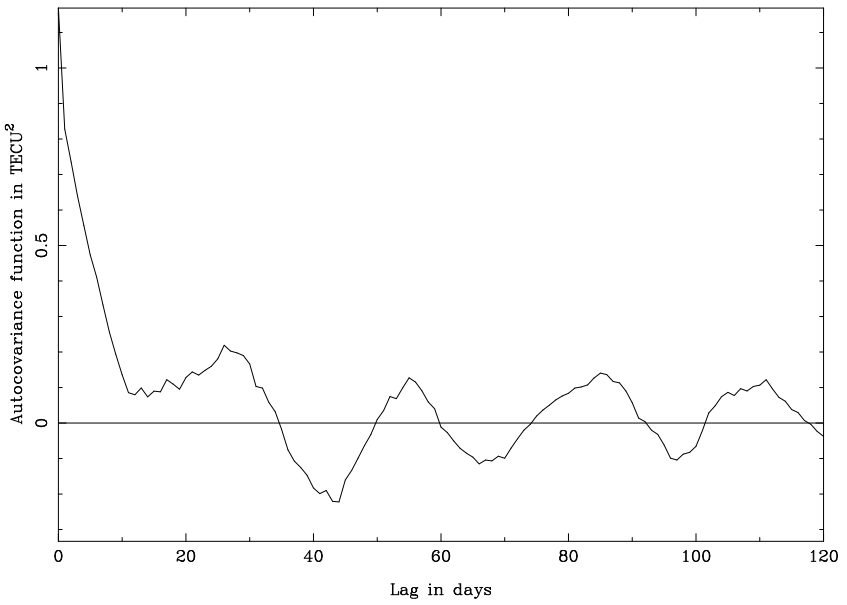

Figure 6. Autocovariance function of zero-degree coefficient for lags up to 120 days

Figure 7 shows the results when predicting (and interpolating) the mean TEC based on (a) a two-year time series *only* and (b) the complete time series. The daily GIM estimates are represented by dots. The trend function $\Phi(t)$ is given by the solid, smooths line and follows the general signal pretty well. It is amazing, considering that the time span of two years is quite short compared to a solar cycle, how well the extrapolated trend function shown in Figure 7a matches the real TEC observations shown in Figure 7b. The rapidly varying line also includes the *stochastic* component covering a prediction length of 30 days.

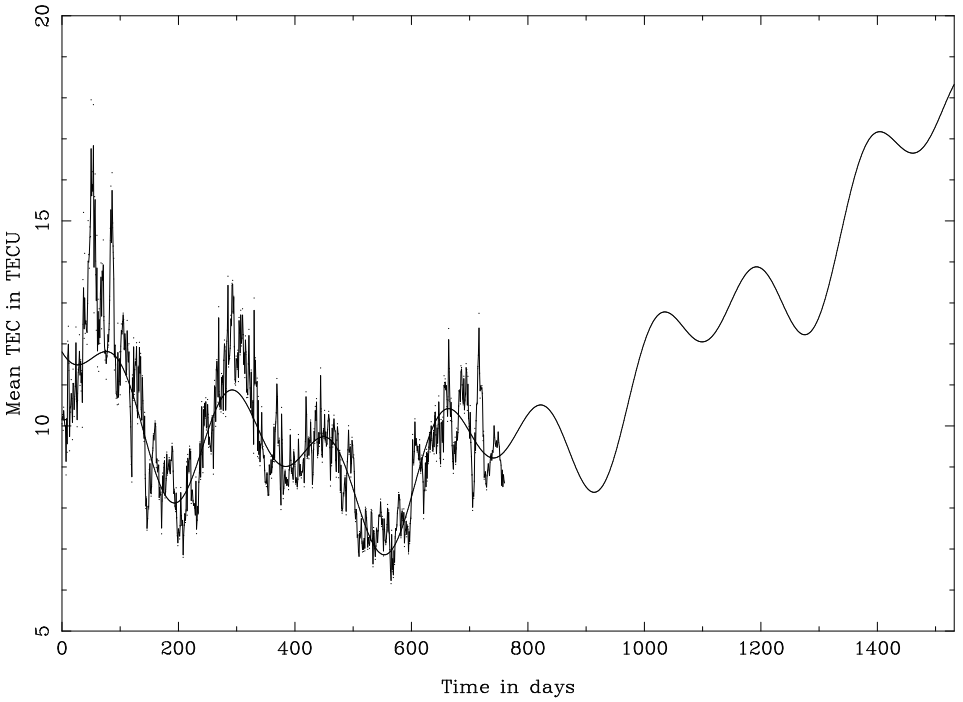

(a) 1995–1996 GIM data

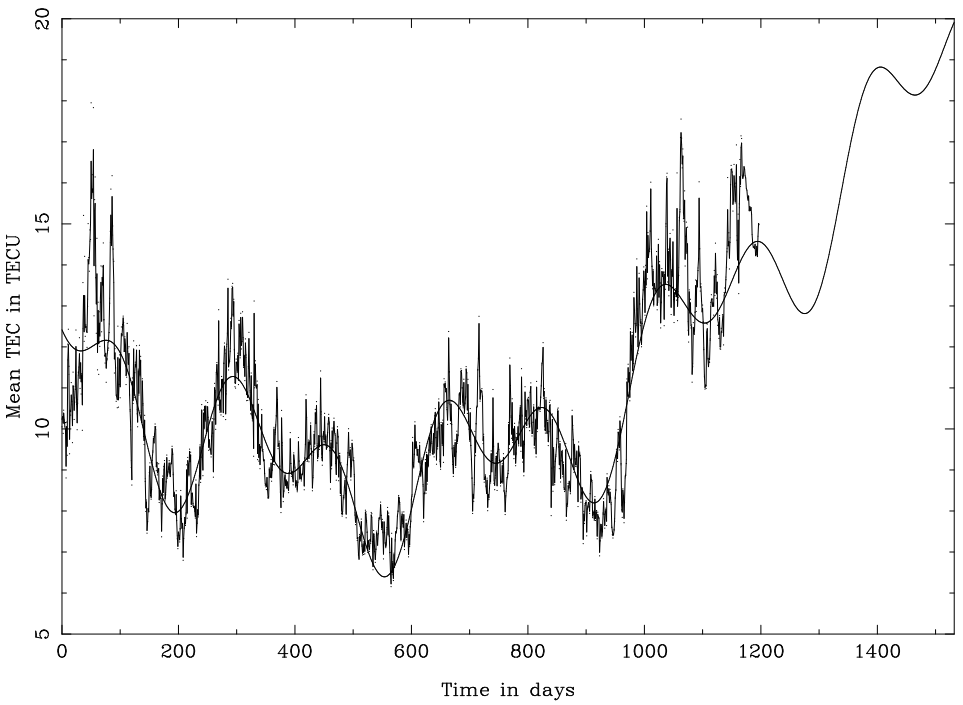

(b) All GIM data

Figure 7. Prediction of mean TEC based on (a) a two-year time series and (b) the complete time series

When inspecting Figure 7 we see that the prediction consisting of $\boldsymbol{d} + \boldsymbol{s}$ does not exactly match the daily estimates because the matrix $\boldsymbol{C}_{nn}$ is not a zero matrix but contains the variances provided by the primary ionosphere parameter estimation.

By performing the least-squares collocation step for each SH coefficient using the same prediction length, merging the predicted TEC coefficients to a full set of SH parameters, and writing a corresponding GIM file, we get a procedure that allows us to predict entire CODE GIMs! A software tool solving that task has been developed.

HIGH TEMPORAL RESOLUTION TEC USING SPHERICAL HARMONIC EXPANSIONS

In this section we discuss a method on how to increase the temporal resolution of the TEC representation when using spherical harmonic (SH) expansion.

SH expansions are well suited to model time-independent quantities given on a spherical surface. When dealing with the ionosphere, the entire sphere is probed by GPS stations when deriving one-day TEC maps. The disadvantage is a poor temporal resolution because of the assumption of a "frozen" ionosphere co-rotating with the Sun. However, the general ionospheric behavior may well be described with daily TEC maps. When generating several TEC maps per day, one has to expect at times unreasonable — very high or negative — TEC estimates in regions where no stations are located. One may avoid such problems by limiting the variations between consecutive TEC maps with "relative" a priori constraints between consecutive maps by adding "relative" pseudo-observations of the type

$$\Delta e_{ij} = e_{ij}(t_k) - e_{ij}(t_{k-1}) = 0 \quad \text{for} \quad k = 2, \ldots, n \tag{7}$$

to the system of normal equations stemming from actual observations. Note that the a priori sigmas $\sigma_{\Delta e_{ij}}$ used for the pseudo-observations Δe_{ij} do not affect the "absolute" TEC determinations. Optimal values for these sigmas have to be found experimentally. Due to the fact that we deal with *normalized* SH coefficients, we may simplify this problem by setting $\sigma_{\Delta e_{ij}} \approx \sigma_{\Delta e}$.

A series of 12 2-hourly TEC maps (taken at 01:00, 03:00, ..., 23:00 UT) is shown in Figure 8a. The typical double-peak structure co-rotating with the Sun fairly well follows the geomagnetic equator, even when referring the TEC representation to a solar-geographic coordinate system. Nevertheless, Figure 8a indicates that a solar-geomagnetic reference frame is more appropriate.

The associated RMS maps shown in Figure 8b describe the formal accuracy of the TEC as a function of earth-fixed coordinates and basically reflect the station coverage. "Light" regions indicate small RMS (see, e. g., Europe or North America), "dark" regions mean large RMS (see, e. g., the region around the station O'Higgens, Antarctica). The ratio of the largest and smallest RMS is about 11. Such RMS maps may be included in IONEX files [Schaer et al., 1998].

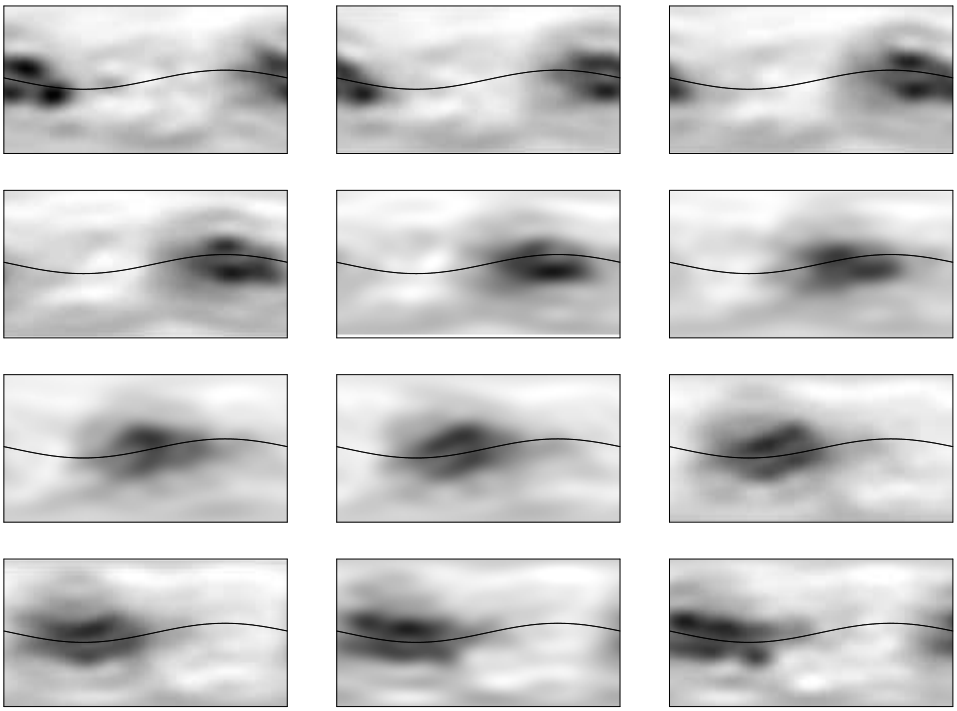

(a) TEC maps

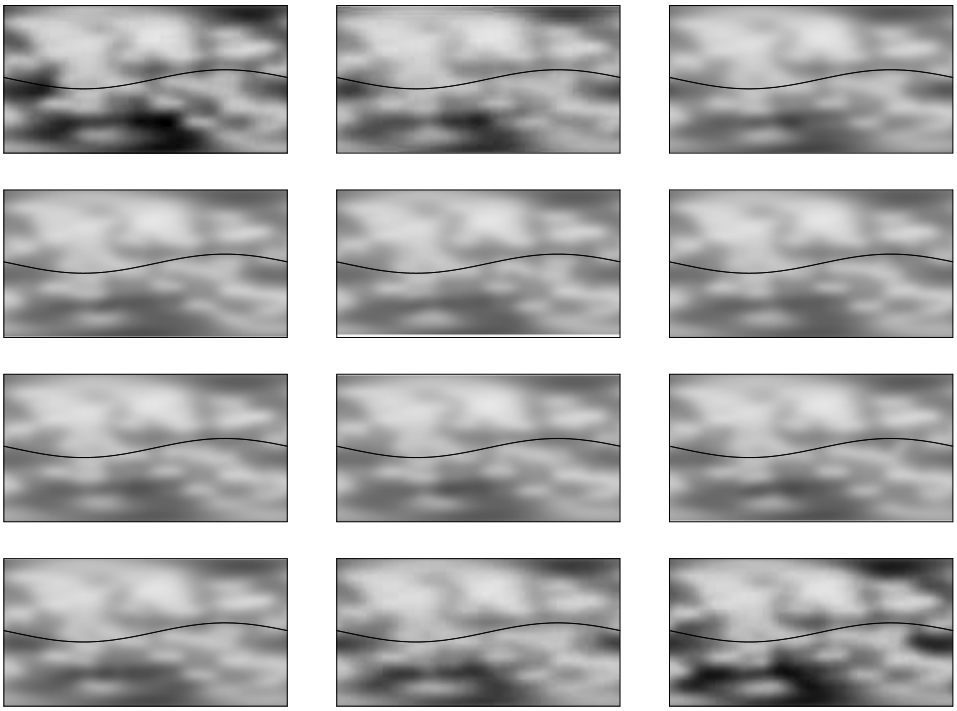

(b) RMS maps

Figure 8. 2-hourly TEC and RMS maps for day 017, 1998

SUMMARY

The CODE Analysis Center produces global and European ionosphere maps by analyzing double-difference phase observations (using an interferometric processing technique) *and* phase-smoothed code observations (processing one-way observations) on a regular basis. Some changes were recently made in our processing scheme: The elevation cut-off angle was decreased from 20 to 10 degrees and at the same time the elevation-dependent observation weighting defining $\cos^2 z$ as weight on the zero-difference level, where z is the zenith distance, was activated. The maximum degree of the SH expansion was increased from 8 to 12 in order to be able to resolve smaller TEC structures like, e. g., the equatorial anomaly.

A higher temporal resolution when using SH expansions is possible by limiting the variations in time with slight "relative" constraints between consecutive sets of SH coefficients. The 2-hour results obtained are very encouraging. The higher the temporal resolution, the less important it is whether a solar-*geographic* or a solar-*geomagnetic* reference frame is used.

Daily sets of differential code biases for the GPS satellites (and receivers) are estimated at CODE since October 1997. The day-to-day scatter of the satellite-specific DCBs is about 0.08 ns. Finally, an approach based on a least-squares collocation to predict global TEC was developed. Approaching the next solar maximum, the knowledge of the ionosphere becomes more and more important. The access to *fast* and *up-to-date* ionospheric information is required by many applications.

OUTLOOK

We will start to produce global ionosphere maps with a 2-hour resolution in the near future. Furthermore we intend to derive predicted ionosphere maps on a regular basis (e. g., 2-day predictions).

The generation of global maps statistically describing the fluctuations of the TEC as presented in [Schaer et al., 1996b] is planned. Reprocessing all global data since 1995 becomes more and more important in view of the progress made in the ionosphere modeling.

It is our declared goal to continuously map the ionosphere for (at least) the next period of high solar activity and to study in particular the impact of the ionosphere on the IGS core products. The establishment of a future IGS ionosphere product as discussed at the IGS AC Workshop in Darmstadt, Germany [Feltens and Schaer, 1998] is another reason to continue these efforts.

REFERENCES

Feltens, J. and S. Schaer, 1998, IGS Products for the Ionosphere, *Proceedings of the IGS AC Workshop*, Darmstadt, Germany, February 9–11, 1998.

Rothacher, M., G. Beutler, E. Brockmann, S. Fankhauser, W. Gurtner, J. Johnson, L. Mervart, S. Schaer, T. A. Springer, and R. Weber, 1996a, *The Bernese GPS Software Version 4.0*, September 1996, Astronomical Institute, University of Berne, Switzerland.

Rothacher, M., G. Beutler, E. Brockmann, L. Mervart, S. Schaer, T. A. Springer, U. Wild, A. Wiget, C. Boucher, and H. Seeger, 1996b, Annual Report 1995 of the CODE Analysis Center of the IGS, *1995 Annual Report of the IGS*, September 1996, IGS Central Bureau, JPL, Pasadena, CA, USA, pp. 151–173.

Schaer, S., G. Beutler, L. Mervart, M. Rothacher, and U. Wild, 1995, Global and Regional Ionosphere Models Using the GPS Double Difference Phase Observable, *Proceedings of the IGS Workshop on Special Topics and New Directions*, Potsdam, Germany, May 15–17, 1995, pp. 77–92.

Schaer, S., G. Beutler, M. Rothacher, and T. A. Springer, 1996a, Daily Global Ionosphere Maps Based on GPS Carrier Phase Data Routinely Produced by the CODE Analysis Center, *Proceedings of the IGS AC Workshop*, Silver Spring, MD, USA, March 19–21, 1996, pp. 181–192.

Schaer, S., M. Rothacher, T. A. Springer, and G. Beutler, 1996b, Mapping the Deterministic and Stochastic Component of the Ionosphere Using GPS, *EOS Transactions of the 1996 AGU Fall Meeting*, Vol. 77, No. 46, p. 142.

Schaer, S., W. Gurtner, and J. Feltens, 1998, IONEX: The IONosphere Map EXchange Format Version 1, February 25, 1998, *Proceedings of the IGS AC Workshop*, Darmstadt, Germany, February 9–11, 1998.